• **Basic Research** •

Effect of intravitreal ranibizumab on fibrovascular membranes in patients with proliferative diabetic retinopathy

Ze−Yu Liang[1], Yi−Peng Wang[2], Jing Li[1], Wen−Chao Yang[2], Yong−Fang Tu[2], Yue Zhang[1], Song Chen[1]

[1]Tianjin Eye Hospital, Tianjin Eye Institute, Tianjin Key Lab of Ophthalmology and Visual Science, Nankai University Affiliated Eye Hospital, Tianjin 300020, China
[2]Anyang Eye Hospital, Anyang 455000, Henan Province, China
Co-first authors: Ze-Yu Liang and Yi-Peng Wang
Correspondence to: Song Chen and Yue Zhang. Tianjin Eye Hospital, Tianjin Eye Institute, Tianjin Key Lab of Ophthalmology and Visual Science, Nankai University Affiliated Eye Hospital, Tianjin 300020, China. chensong9999@126.com; zhangmoon0225@126.com
Received: 2022-05-16　　Accepted: 2022-08-12

Abstract

● **AIM:** To assess the effects of intravitreal ranibizumab (IVR) on angiogenesis and glial activity of the fibrovascular membrane (FVM) in patients with proliferative diabetic retinopathy (PDR).

● **METHODS:** Forty-two eyes from 42 patients with PDR requiring vitrectomy were included and divided into two groups: control group (n=16) did not receive IVR, while IVR group (n=26) underwent IVR 5d before vitrectomy. FVM specimens were collected by the same surgeon during the interventions. Histopathological morphology was examined by hematoxylin-eosin (H-E) staining and cell densities in the FVM was assessed. Microvessels were outlined by immunohistochemical staining of CD31 and microvessel density (MVD) assessed as an index of FVM angiogenesis. Dual-color immunofluorescence staining, and confocal microscopy was used to detect co-localization and relative expression levels of glial fibrillary acidic protein (GFAP) and α-smooth muscle actin (α-SMA) as markers of glial-mesenchymal transition (GMT). The GMT index (GI; ratio of relative GFAP/α-SMA expression) was used to semi-quantify the degree of GMT or glial activity of FVMs.

● **RESULTS:** H-E staining showed similar vascularization in both groups, with microvessels and scattered stromal cells in the matrix. Infiltrated cell densities did not differ significantly between the two groups (P>0.05). The MVD of the IVR group (130.62±15.46/mm^2) was significantly lower than that of the controls (142.25±19.16/mm^2, P<0.05). In both groups, all sections were strongly immunostained for GFAP and α-SMA. The Pearson's correlation coefficients (PCC) of intensity of automated pixel count of two markers indicated GFAP and α-SMA co-stained well and GMT participated in the remolding of FVMs in PDR. The mean relative GFAP expression in the IVR group was significantly lower, whereas that of α-SMA was significantly higher than in controls (P<0.05). GI in the IVR group (1.10±0.10) was significantly lower than in the controls (1.21±0.12, P<0.05).

● **CONCLUSION:** IVR can reduce angiogenesis, glial activity of FVM and promote glial-fibrotic transformation by reducing MVD and promoting GMT but does not decrease the cell density in patients with PDR.

● **KEYWORDS:** proliferative diabetic retinopathy; ranibizumab; fibrovascular membranes; glial-mesenchymal transition; microvessel density

INTRODUCTION

I n patients with proliferative diabetic retinopathy (PDR), fibrovascular membranes (FVMs) are characterized by abnormal neovascularization, combined with extracellular matrix (ECM) containing infiltrated cells[1]. The remodeling and pathology of FVMs can be understood as a scar-like repair procedure, involving multiple interactions among processes, including angiogenesis, glial activity, inflammatory cell infiltration, matrix metalloproteinases, and fibrosis[2-3]. Glial or fibrocyte-like cells originating from the retina or posterior vitreous cortex are components of the FVM in PDR[4-5]. Compared with active FVMs, inactive fibrosis epiretinal

membranes exhibit more fibrotic stroma combined with less angiogenesis or proliferation, and are the indicator of less active condition of PDR and lower levels of inflammation, in which condition the vitrectomy was performed more easier[6-7]. Several factors can be used to evaluate FVM activity. First, autocrine vascular endothelial growth factor (VEGF) in Müller/glial cells is activated by tractive force or fluctuations caused by the FVM, influencing VEGF concentration in vitreous fluid in PDR[8]. Abnormally high expression of VEGF combined with other cytokines in the vitreous cavity can stimulate Müller/glia cells to express high levels of glial fibrillary acidic protein (GFAP) in turn. Thus, GFAP levels in the FVM or retina can indicate the active state of PDR[9-10]. Furthermore, the density of infiltrated lymphocyte cells is correlated with inflammation of FVM in PDR[11]. Therefore, microvessel density, infiltrated cells, and GFAP expression in FVMs are positively correlated with the PDR stage.

There are pathological conditions that involve the transformation of active FVMs into inactive membranes. This transformation of cells into myofibroblasts is the classic pathology of fibrosis in FVM, and myofibroblasts are key cells accumulated in the ECM, while α-smooth muscle actin (α-SMA), which contributes to the contractive force of FVMs on the retina, is a classic and reliable marker of mesenchymal and myofibroblast differentiation[12-13]. Similar to the canonical concept of angio-fibrotic transformation, where vascular endothelial cells are transformed into myofibroblasts by the pathological endothelial to mesenchymal transition (EMT) of vessels in FVM[14], glial cells in FVM are also involved in fibrogenic dedifferentiation, defined as glial-mesenchymal transition (GMT). The GMT is characterized by down-regulation of GFAP expression and up-regulation of α-SMA, and is considered a subcategory of EMT involving glial cells that contribute to fibrosis in FVM[15]. In summary, the transformation of glial activation into fibrotic proliferation in the FVM participates in FVM remodeling; hence, by evaluating the relative expression levels of GFAP and α-SMA, we can analyze the degree of shift of glial activity towards fibrosis in FVMs.

Pretreatment by intravitreal injection of VEGF inhibitor drugs as an adjunct to vitrectomy in PDR patients with activated FVM has highlighted the ability of this approach to facilitate surgical interventions or improve the outcomes of vitrectomies and has already been proved for not aggravating tractional retinal detachment in short time[16-17]. Previous research has focused mainly on the pathogenesis or histology of angiogenesis in epiretinal membranes of patients with PDR; however, questions arise as to whether short-term inhibition of VEGF accelerates the glial-fibrotic change in FVMs of patients with PDR. The aim of this study was to explore the effect and underlying mechanisms of intravitreal injection of ranibizumab, a monoclonal antibody fragment that binds to the VEGF-A isoform, on angiogenic and glial activity in FVMs, with a particular focus on GMT, in tissues excised from patients with PDR.

SUBJECTS AND METHODS

Ethical Approval The research protocols for this randomized clinical control study were approved by the institutional review board of Tianjin Eye Hospital and the study adhered to the tenets of the Declaration of Helsinki for the collection of both specimens and clinical data for subsequent analysis. All of the patients included in this study provided informed consent.

Study Population From October 2019 to August 2020, all patients with PDR with tractional retinal detachment (TRD) requiring vitrectomy were included in the study, provided that the details of the fundus could be clearly visualized and FVMs were present. Patients were excluded if they had quiescent epiretinal membrane fibrosis (no obvious vessels) fibrosis of epiretinal membranes, any previous history of intravitreal injection of anti-VEGF drugs, a history of surgery, pan-retinal photocoagulations during the last three months, or any poorly controlled systematic disease.

Patient Examination and Sample Collection All of the 42 patients with PDR (42 affected eyes) included in this study received best-corrected visual acuity (BCVA) by standard logarithmic visual acuity chart, slit lamp examination, fundus examination, and intraocular pressure measurement before pars plana vitrectomy (PPV). Patients were grouped based on whether they received an intravitreal injection of ranibizumab (IVR) prior to vitrectomy surgery by the principle of voluntariness: Patients in the IVR group received ranibizumab (0.5 mg) 5d before vitrectomy and the control group with not any an intravitreal injection. The FVM tissues were surgically removed from the vitreous cavity using end-gripping forceps and fixed in buffered 4% paraformaldehyde and then embedded in paraffin for at least 24h. Paraffin-embedded tissues were cut into at least five 4-μm sections, of which one was selected for hematoxylin-eosin (H-E) staining and the remaining four serial sections were used equally to perform immunohistochemical staining for CD31 and dual immunofluorescence histochemistry staining for GFAP and α-SMA.

Histological Analysis Three serial fields were captured in one section at the stated magnification by light microscopy for subsequent analysis. The method described by Jiao et al[18] was used to quantify the density of nucleated cells in H-E stained FVM sections under high-power (×400) microscopy with Image J software. Colored images were converted to 8-bit grayscale and all images were subjected to the same threshold and binary images analysis. Image areas were measured in mm^2, with pixel conversion according to the scale and

magnification of the light microscope. Nucleated cell density is expressed as the mean number of cells per mm^2 (/mm^2).

Immunohistochemical Analysis For immunohistochemistry, tissue sections were incubated overnight at 4□ with mouse monoclonal anti-CD31 antibody (1:50, Abcam). First sections were deparaffinized, dehydrated, and any endogenous peroxidase activity was eliminated by incubating in 3% H$_2$O$_2$ in methanol, and subjected to heat-induced antigen retrieval, and then incubated with diluted normal rabbit serum (1:10) overnight at 4□. The following day, sections were incubated in biotinylated secondary antibody for 1h and the bound antibody was visualized using the peroxidase substrate, diaminobenzidine, according to the manufacturer's instructions. Hematoxylin was used as a counterstain. Images were captured using an Olympus BX41 light microscope.

Evaluation of Microvessel Density Evaluation of microvessel density (MVD) was based on the method of Weidner[19]. The microvessel outlines were visualized by staining for CD31, a marker of vascular endothelial cells. Capillaries were located in low power fields (10×10), then at least three representative fields were selected for high-power examination (HP, 40×10; area, 0.24 mm^2; number of fields, 22) to count the number of microvessels covering the entire stromal area, excluding large vessels with lumen diameter >50 μm. Any single layer of brown-stained endothelial cells separated from other microvessels or connective tissues was considered a countable microvessel. MVD was calculated as the mean number of vessels per HP area (/mm^2). Two investigators were blinded to the details of the groups, their combined their data was used for statistical analysis.

Dual-color Immunofluorescence Staining GFAP and α-SMA, as markers of activated glial cells and myofibroblasts, respectively, were analyzed by dual-color immunofluorescence staining to detect their co-localization and relative expression levels. Cells positive for both GFAP and α-SMA were considered glia-derived myofibroblasts undergoing GMT[15]. The GMT index (GI) of FVM was calculated as the ratio of the relative expression of GFAP and α-SMA expression to semi-quantify GMT activity in FVMs.

Indirect immunofluorescence was analyzed according to the method described by Jiao *et al*[18]. The sections were deparaffinized and dehydrated and then incubated with each of the following primary antibodies sequentially for 60min: mouse-anti-α-SMA (1:100; Abcam) and rabbit-anti-GFAP (1:100; Abcam). Next, the samples were washed three times for 5min with phosphate buffered saline (PBS) and incubated with Alexa Fluor 647 goat anti-mouse IgG (1:100; Abcam) and Alexa Fluor 488 goat anti-rabbit IgG (1:100; Abcam). The sections were then washed three times with PBS after each incubation step and then mounted with 4',6-diamidino-2-

phenylindole (1:1000; Abcam). All images were examined and photographed within 24h to prevent fluorescence quenching, using a fluorescent microscope under the same parameters (Leica DM4000 B LED, Germany). At least three exposures for both antigens were evaluated for each sample.

The mean marked tissue-associated gray value, calculated as the ratio of the integrated density to the area of the image[20], was conducted to provide a semi-quantitative analysis of protein expression. Colored images were converted to 8-bit type and Red-Default mode, so that the positive area stained red on a dark background. The built-in Image J Colocalization Finder software was used to evaluate the colocalization of the two proteins stained by dual color immunofluorescence and was assess using the Pearson's correlation coefficient (PCC) for the correlation between the intensity of the pixel count intensity of the two markers. PCC values closer to 1 indicated a stronger colocalization of the pixel intensities of markers[21].

Statistical Analysis Statistical analyses were performed using SPSS 24 software. Quantitative data are presented as mean±standard deviation (SD) or median, according to their distribution. Comparisons of sample rates were performed using the Chi-square test. The Student's *t*-test was used to compare differences between two groups if data were normally distributed with equal variance. Data were analyzed by Mann-Whitney *U* test for populations with non-normal distributions or unequal variance. *P* values <0.05 were considered statistically significant.

RESULTS

Demographic and Clinical Characteristics of the Study Groups There were no significant differences with regard to relevant clinical data between the two groups (all *P*>0.05; Table 1).

Morphometric Analysis, Cell Intensity, and Microvessel Density Evaluation H-E staining showed that all FVM tissue samples from both groups were vascularized with numerous microvessels or scattered stromal cells in fibrotic membranes. The microvessels exhibited irregular vascular structures, combined with a single layer of perivascular cells with large nuclei (Figure 1).

The mean cell density of FVM in the control group was (1095.38±160.00)/mm^2, which was slightly higher than that of the IVR group (1037.46±144.49)/mm^2, although the difference was not significant (*P*>0.05; Figure 1, Table 2).

The mean MVD values in the control and IVR groups were (142.25±19.16) and (130.62±15.46)/mm^2, respectively, representing significantly higher MVD in the IVR group (*P*<0.05; Figure 2, Table 2).

Glial-Mesenchymal Transition in Fibrovascular Membranes All tested sections from both groups were strongly immunostained for both GFAP and α-SMA. The
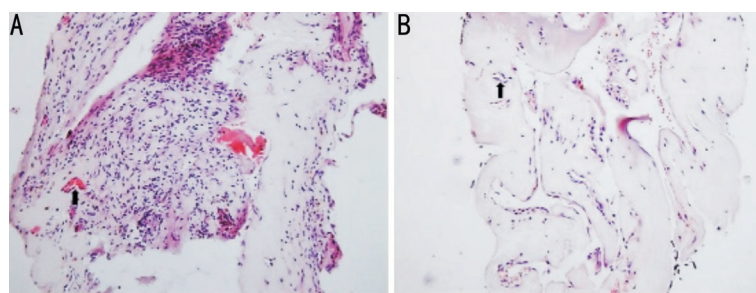
Figure 1 Histological analysis of fibrovascular membrane samples from patients with proliferative diabetic retinopathy H-E stained sections of the control group (A) and the IVR group (B) showing FVM visualized by light microscopy (×100; scale bar, 100 μm) and changes in the histological morphology of FVMs in patients treated with or without ranibizumab. Arrows indicate microvessels and many cells are visible infiltrated in the stroma. There was no significant difference in infiltrated cells between the two groups (P>0.05). IVR: Intravitreal ranibizumab; FVM: Fibrovascular membrane; H-E: Hematoxylin-eosin.

Table 1 Clinical and demographic characteristics of study participants

Characteristics	Control (n=16)	IVR (n=26)	P
Age (y), mean±SD	54.75±9.15	55.38±7.69	0.810
Sex, n (%)			0.694
Male	9 (56.3)	13 (50)	
Female	7 (43.8)	13 (50)	
Duration of diabetes (mo), mean±SD	8.56±2.92	6.77±3.17	0.074
PRP, n (%)			0.303
Yes	6 (37.5)	14 (53.8)	
No	10 (62.5)	12 (46.2)	
Insulin administration, n (%)			1.000
Yes	13 (81.3)	21 (80.8)	
No	3 (18.8)	5 (19.2)	
Type of diabetes[a], n (%)			1.000
Type 1	4 (40)	6 (15)	
Type 2	12 (60)	20 (85)	
Preoperative BCVA (logMAR), median (range)	1.28 (0.52, 3.0)	1.47 (0.7, 3.0)	0.33
Preoperative IOP (mm Hg)	18.25±3.17	17.19±3.24	0.306

[a]Type 1: Insulin-dependent diabetes mellitus; Type 2: Non-insulin-dependent diabetes mellitus; IVR: Intravitreal ranibizumab; PRP: Pan-retinal photocoagulations; BCVA: Best corrected visual acuity; IOP: Intraocular pressure.

Table 2 Comparison of cell density and MVD of FVM in the two groups

Parameters	Control (n=16)	IVR (n=26)	F	P
Cells density (/mm^2)	1095.38±160.00	1037.46±144.49	0.333	0.233
MVD (/mm^2)	142.25±19.16	130.62±15.46	0.531	0.037

IVR: Intravitreal ranibizumab; FVMs: Fibrovascular membranes; MVD: Microvessel density.

mean PCC values of the two markers in the control group were 0.764±0.08 and 0.783±0.06, respectively. There were no significant differences between the two groups, and the two markers were strongly co-localized in both groups (P>0.05). Areas of positive staining for GFAP and α-SMA were mainly cells scattered within the stroma, but there was also staining of vessel walls. These data support the hypothesis that GMT is involved in the pathology of FVM (Figure 3).

Effect of VEGF Inhibition on Glial-Mesenchymal Transition of Fibrovascular Membranes The expression of GFAP and α-SMA expression differed significantly between the two groups, with the expression of GFAP significantly lower (P<0.05) and α-SMA significantly higher in the IVR group (P<0.05; Figures 4 and 5). The mean GI in the IVR group was 1.10±0.10, which was significantly lower than in the control group (1.21±0.12, P<0.01), indicating that the IVR can down-regulate glial activity and accelerate fibrosis in FVM through GMT pathology (Figure 6).

DISCUSSION

In this study, we confirmed that activated glial cells and GMT participate in the formation of FMVs in PDR. Additionally, we discovered that IVR has positive effects on vessel regression by
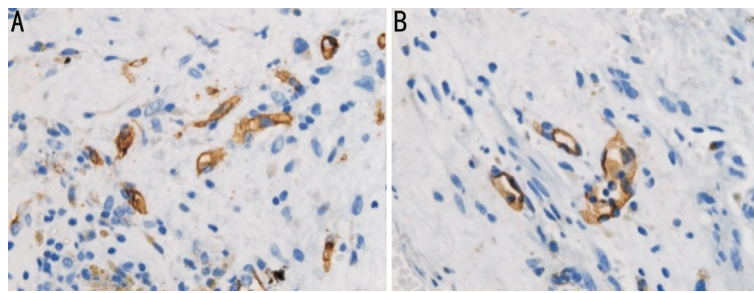
Figure 2 Immunohistochemical analysis by light microscopy Differences in MVD between the control group (A) and IVR group (B). Microvessel outlines are highlighted by staining for the vascular endothelial cell marker, CD31. MVD was evaluated in areas containing the most discrete vessels by counting the number per 400× field (×400; scale bar, 25 μm). IVR: Intravitreal ranibizumab; MVD: Microvessel density.
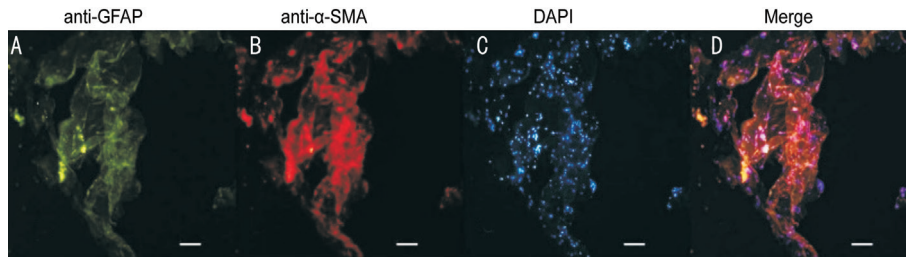

Figure 3 Expression and colocalization of two markers of the glial-mesenchymal transition in FVM samples from patients with proliferative diabetic retinopathy GFAP (A, green) and α-SMA (B, red), were strongly immunostained and co-localized in the FVM (D). Nuclei were labeled with DAPI (C, blue). GFAP$^+$/α-SMA$^+$ cells were spindle-shaped and distributed in the stroma; however, there was also positive staining of the vessel walls (×200; scale bar, 50 μm). FVM: Fibrovascular membrane; GFAP: Glial fibrillary acidic protein; α-SMA: α-smooth muscle actin.
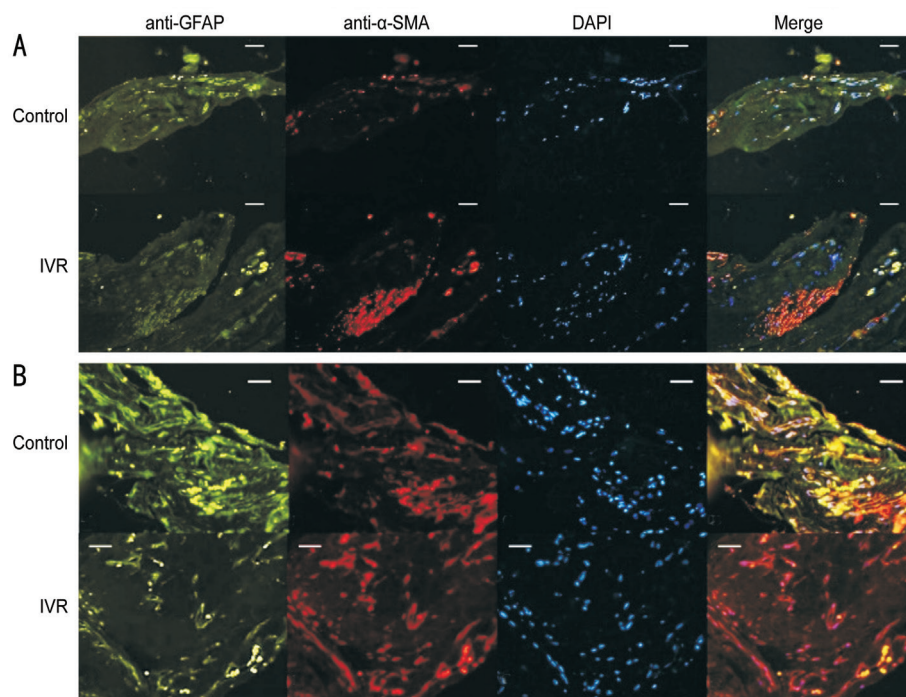

Figure 4 Immunofluorescence analysis of markers of the glial mesenchymal transition in fibrovascular membrane samples from patients with proliferative diabetic retinopathy A: ×200; scale bar, 50 μm; B: ×400; scale bar, 25 μm.

reducing MVD, downregulating glial activity, and promoting GMT, thus alleviating GI; however, no change in cell density was observed in FVM in response to inhibition of VEGF. Anti-VEGF agents can down-regulate inflammatory cell infiltration by restoring tight junctions between vascular endothelial cells or pericytes in the retina or cornea during pathological conditions[22-23]. Jiao *et al*[18] demonstrated that bevacizumab, an anti-VEGF agent, induces apoptosis of cells within FVMs, while cell counts were not significantly alleviated, consistent with our conclusion. We did not detect
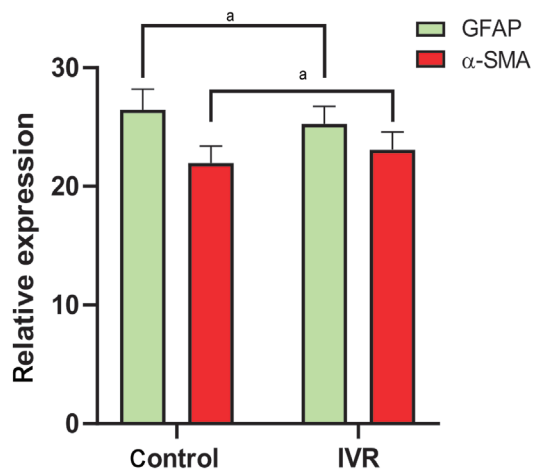
Figure 5 Differences in the relative expression levels of GFAP and α-SMA in the two groups Relative expression of GFAP was significantly higher, and that of α-SMA significantly lower, in the control group relative to the IVR group. Student's *t*-test was used for statistical analysis, [a]$P<0.05$. IVR: Intravitreal ranibizumab; GFAP: Glial fibrillary acidic protein; α-SMA: α-smooth muscle actin.
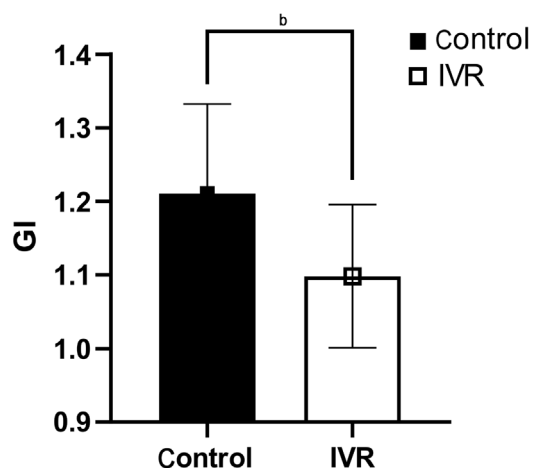

Figure 6 Comparison of the glial-mesenchymal transition index (GI) between the two groups The mean GI in the IVR group was (1.10±0.10), which was significantly lower than in the control group (1.21±0.12). [b]$P<0.01$. IVR: Intravitreal ranibizumab.

any effect of IVR on FVM cell density, likely because cell density was evaluated by H-E staining, which shows only cell nuclei, rather than apoptotic cells. Furthermore, in FMV tissues, local cells were mainly hyalocytes, myofibroblasts, fibroblasts, and an abundance of glial cells migrated from the posterior vitreous cortex or the superficial retina, rather than leaking from the capillaries or micro vessels in retina or FVMs[4,24].

VEGF concentration in vitreous fluid is a classic marker for evaluating angiogenesis activity in PDR[25]. MVD, a quantitative index of neovascularization used to evaluate angiogenesis activity and tumor intravasation[26], has also been applied to assess FVM activity in PDR[27]. We selected CD31 as a marker of mature vascular endothelial cells, rather than

CD34, which is used to identify mesenchymal-derived vascular endothelial progenitors or peripheral hematopoietic cells[28-29], to outline vessels and calculate MVD. In our study, we found that the mean MVD in the control group was $(142.25\pm19.16)/mm^2$, while Abu El-Asrar *et al*[27,30] reported MVD values in FVM of 122.5±44.6 or 70.0±14.3 in an area of 0.33×0.22 mm^2 in patients with active PDR and neovascularized optic discs, which are relatively high compared to our findings. Furthermore, Tsanou *et al*[9] reported MVD values of 10.8 per high-power magnification (×400) in FVMs. These differences probably reflect variation in the proliferative stage of the PDR when tissues were collected.

Nakao *et al*[31] revealed that intravitreal injection of bevacizumab (IVB) alleviated blood density by decreasing the intraluminal area of blood vessels compared to untreated FVM. Regarding the mechanism underlying the inhibitive effect of anti-VEGF therapy on the MVD of FMV, they concluded that VEGF inhibition can induce vessel contraction, rather than vessel regression. Our study also showed that MVD decreased after inhibition of VEGF, revealing that ranibizumab can alleviate angiogenesis activity in FVM, similar to the conclusions of previous studies that intravitreal injections of anti-VEGF drugs can reduce VEGF expression or vascular density in active FVM of patients with PDR[32-34]. Kohno *et al*[35] showed that IVB 2d before vitrectomy regress vessels by inducing vascular endothelial cell apoptosis in FVMs of patients with PDR. In addition to histological observations, Hu *et al*[36] quantified the regression of neovascularization using optical coherence tomography angiography and observed a plateau of blood flow regression 3d after intravitreal injection of conbercept, another anti-VEGF drug. Contrary to our approach, Nakao *et al*[31] selected CD34 to evaluate MVD of MVD of FVM in patients with PDR and found no significant reduction in MVD 4 to 14d after IVB; however, VEGF immunoreactivity decreased significantly in FVMs after IVB, relative to control eyes treated with PRP only. Thus, the authors speculated that inhibition of VEGF temporally reduces blood flow in new vessels and alleviates vessel leakage by reducing fenestrations between vascular endothelial cells, rather than reducing the structures of detectable capillaries described histologically[31]. Furthermore, the conclusions of Pattwell *et al*[37] also did not support the phenomenon of vessel regression in FVM after IVB, and their findings revealed that side effects of the vasoconstrictive response to anti-VEGF therapy can increase the constrictive force of FVM. These authors observed that blood-containing lumens were still present after IVB; however, they did not assess the number of vessels and did not provide details of the patient's history of pan retinal photocoagulation therapy. Based on all the findings discussed above, we speculate that the short-term effects of IVR on FVM angiogenesis include temporary

reduction in blood flow combined with alleviation of MVD, likely through vessel vasoconstriction and reduced expression of CD31 caused by EMT, combined with induction of vascular endothelial cell apoptosis in FVM[14].

GFAP immunoreactivity is positively correlated with glial activity or epiretinal membrane gliosis[4]. Consequently, activated Müller cells have the potential to transform into myofibroblasts, characterized by downregulation of GFAP combined with increased de novo α-SMA expression, demonstrating that GMT participates in fibrotic transformation and contributes to the formation of contractive forces in the retina[38-39]. We also found that GMT participates in the pathology of FVM in patients with PDR, based on the strong colocalization of GFAP and α-SMA. We did not investigate further the origins of GFAP⁻positive cells in FVMs. A previous study showed that GFAP-positive cells in epiretinal membranes (ERM) were not pure glial cells and that some of them expressed progenitor cell markers, indicating the potential for self-renewal[40]. Regarding the phenotype of glial cells, previous studies have demonstrated that GFAP immunoreactivity is observed primarily in activated Müller cells or glial cells, and generally not in microglia cells, as these originate from macrophages that do not express GFAP in FVMs of patients with PDR[41-42].

Our findings indicate that IVR reduces glial activity, promotes GMT, and leads to the maturation of FVM in PDR, by alleviating GI. The mean GI value of active FVM in controls was 1.21±0.12, on the contrary, the GI was 1.10±0.10 in IVR group, revealing an accelerated glial-fibrotic shift in FVMs after anti-VEGF therapy. In an evaluation of the degree of GMT and influencing factors, Krishna Chandran et al[43] reported that vitreous components play a critical role in GMT in idiopathic ERMs (iERMs). They classified iERM into two forms according to the relative expression of GMT genes, and demonstrated that iERM undergoing partial GMT were associated with more severe clinical and Spectral domain-optical coherence tomography (SD-OCT) features than those undergoing complete GMT, with upregulation of genes encoding cell proliferation and a lack of clear regulation of genes encoding mesenchymal markers, such as α-SMA, in complete GMT, with consistent downregulation of *GFAP*-encoding Müller cell/glial markers, in parallel with upregulation of myofibroblast markers[43]. Thus, we infer that elevated α-SMA expression is correlated with less proliferative or glial activity and greater improvement of epiretinal membrane pathology. In this study, we found that FVMs tended to be closer to complete GMT after IVR therapy. Regarding the underlying mechanism, the promotion of gliosis of activated glial cells into fibrosis is induced by cytokines or profibrotic factors in the microenvironment[44-45]. Anti-VEGF

agents cause structural protein abnormalities in cultured Müller cells, with decreased levels of GFAP and vimentin, probably due to the VEGF family receptors expressed in Müller cells[46-47]. Another way in which IVR can promote GMT is the neutralizing influence of VEGF on the inductive effects of released profibrotic factors, such as transforming growth factor (TGF)-β[48-49], which is supported by previous studies showing that α-SMA or fibronectin in myofibroblasts depends on profibrotic cytokines, and that GMT in diabetic fibrovascular proliferation is driven by autoinduction of TGF-β in Müller glial cells[15,50].

In conclusion, our study describes the histological changes in FVM in patients with PDR after IVR and demonstrates that IVR can reduce FVM angiogenesis and glial activity by alleviating MVD and stimulating GMT characterized by regulation of the gastrointestinal system. A deeper understanding of these processes could shed light on molecular signaling pathways or profibrotic cytokines involved in the promotion of GMT.

REFERENCES

1 Pouw AE, Greiner MA, Coussa RG, Jiao CH, Han IC, Skeie JM, Fingert JH, Mullins RF, Sohn EH. Cell-matrix interactions in the eye: from cornea to choroid. *Cells* 2021;10(3):687.

2 Yu Y, Bao ZY, Wang XF, Gong WH, Chen H, Guan HJ, Le YY, Su SB, Chen KQ, Wang JM. The G-protein-coupled chemoattractant receptor Fpr2 exacerbates high glucose-mediated proinflammatory responses of Müller glial cells. *Front Immunol* 2017;8:1852.

3 Hu YG, Xie AM, Cheng QC. Upregulated CD200 in pre-retinal proliferative fibrovascular membranes of proliferative diabetic retinopathy patients and its correlation with vascular endothelial growth factor. *Inflamm Res* 2019;68(12):1071-1079.

4 Kim LA, Wong LL, Amarnani DS, Bigger-Allen AA, Hu Y, Marko CK, Eliott D, Shah VA, McGuone D, Stemmer-Rachamimov AO, Gai XW, D'Amore PA, Arboleda-Velasquez JF. Characterization of cells from patient-derived fibrovascular membranes in proliferative diabetic retinopathy. *Mol Vis* 2015;21:673-687.

5 Chang W, Lajko M, Fawzi AA. Endothelin-1 is associated with fibrosis in proliferative diabetic retinopathy membranes. *PLoS One* 2018;13(1):e0191285.

6 Jo DH, Yun JH, Cho CS, Kim JH, Kim JH, Cho CH. Interaction between microglia and retinal pigment epithelial cells determines the integrity of outer blood-retinal barrier in diabetic retinopathy. *Glia* 2019;67(2):321-331.

7 Mao JB, Wu HF, Chen YQ, Zhao SX, Tao JW, Zhang Y, Zheng B, Wang L, Shen LJ. Effect of intravitreal conbercept treatment before

vitrectomy in proliferative diabetic retinopathy. *Int J Ophthalmol* 2018;11(7):1217-1221.

8 Patel JI, Tombran-Tink J, Hykin PG, Gregor ZJ, Cree IA. Vitreous and aqueous concentrations of proangiogenic, antiangiogenic factors and other cytokines in diabetic retinopathy patients with macular edema: implications for structural differences in macular profiles. *Exp Eye Res* 2006;82(5):798-806.

9 Tsanou E, Ioachim E, Stefaniotou M, Gorezis S, Charalabopoulos K, Bagli H, Peschos D, Psilas K, Agnantis NJ. Immunohistochemical study of angiogenesis and proliferative activity in epiretinal membranes. *Int J Clin Pract* 2005;59(10):1157-1161.

10 Le YZ. VEGF production and signaling in Müller glia are critical to modulating vascular function and neuronal integrity in diabetic retinopathy and hypoxic retinal vascular diseases. *Vis Res* 2017;139: 108-114.

11 Kase S, Saito W, Ohno S, Ishida S. Proliferative diabetic retinopathy with lymphocyte-rich epiretinal membrane associated with poor visual prognosis. *Invest Ophthalmol Vis Sci* 2009;50(12):5909-5912.

12 Fischer AJ, Reh TA. Potential of Müller glia to become neurogenic retinal progenitor cells. *Glia* 2003;43(1):70-76.

13 Korhonen A, Gucciardo E, Lehti K, Loukovaara S. Proliferative diabetic retinopathy transcriptomes reveal angiogenesis, anti-angiogenic therapy escape mechanisms, fibrosis and lymphatic involvement. *Sci Rep* 2021;11(1):18810.

14 Abu El-Asrar AM, de Hertogh G, van den Eynde K, Alam K, van Raemdonck K, Opdenakker G, van Damme J, Geboes K, Struyf S. Myofibroblasts in proliferative diabetic retinopathy can originate from infiltrating fibrocytes and through endothelial-to-mesenchymal transition (EndoMT). *Exp Eye Res* 2015;132:179-189.

15 Kanda A, Noda K, Hirose I, Ishida S. TGF-β-SNAIL axis induces Müller glial-mesenchymal transition in the pathogenesis of idiopathic epiretinal membrane. *Sci Rep* 2019;9:673.

16 Al Sarireh F, Alrawashdeh HM, Al Zubi K, Al Salem K. Role of bevacizumab intraocular injection in the management of neovascular glaucoma. *Int J Ophthalmol* 2021;14(6):855-859.

17 Wang DY, Zhao XY, Zhang WF, Meng LH, Chen YX. Perioperative anti-vascular endothelial growth factor agents treatment in patients undergoing vitrectomy for complicated proliferative diabetic retinopathy: a network meta-analysis. *Sci Rep* 2020;10(1):18880.

18 Jiao CH, Eliott D, Spee C, He SK, Wang K, Mullins RF, Hinton DR, Sohn EH. Apoptosis and angiofibrosis in diabetic tractional membranes after vascular endothelial growth factor inhibition: results of a prospective trial. report no. 2. *Retina* 2019;39(2):265-273.

19 Weidner N. Current pathologic methods for measuring intratumoral microvessel density within breast carcinoma and other solid tumors. *Breast Cancer Res Tr* 1995;36(2):169-180.

20 Jensen EC. Quantitative analysis of histological staining and fluorescence using ImageJ. *Anat Rec* (*Hoboken*) 2013;296(3): 378-381.

21 Dunn KW, Kamocka MM, McDonald JH. A practical Guide to evaluating colocalization in biological microscopy. *Am J Physiol Cell Physiol* 2011;300(4):C723-C742.

22 Chen WL, Chen YM, Chu HS, Lin CT, Chow LP, Chen CT, Hu FR. Mechanisms controlling the effects of bevacizumab (avastin) on the inhibition of early but not late formed corneal neovascularization. *PLoS One* 2014;9(4):e94205.

23 Cam D, Berk AT, Micili SC, Kume T, Ergur BU, Yilmaz O. Histological and immunohistochemical retinal changes following the intravitreal injection of aflibercept, bevacizumab and ranibizumab in newborn rabbits. *Curr Eye Res* 2017;42(2):315-322.

24 Vogt D, Vielmuth F, Wertheimer C, Hagenau F, Guenther SR, Wolf A, Spindler V, Priglinger SG, Schumann RG. Premacular membranes in tissue culture. *Graefes Arch Clin Exp Ophthalmol* 2018;256(9): 1589-1597.

25 Keles A, Sonmez K, Erol YO, Ayyıldız SN, Ogus E. Vitreous levels of vascular endothelial growth factor, stromal cell-derived factor-1α, and angiopoietin-like protein 2 in patients with active proliferative diabetic retinopathy. *Graefes Arch Clin Exp Ophthalmol* 2021;259(1):53-60.

26 Chiang SPH, Cabrera RM, Segall JE. Tumor cell intravasation. *Am J Physiol Cell Physiol* 2016;311(1):C1-C14.

27 Abu El-Asrar AM, Ahmad A, Allegaert E, Siddiquei MM, Gikandi PW, De Hertogh G, Opdenakker G. Interleukin-11 overexpression and M2 macrophage density are associated with angiogenic activity in proliferative diabetic retinopathy. *Ocul Immunol Inflamm* 2020;28(4):575-588.

28 Sidney LE, Branch MJ, Dunphy SE, Dua HS, Hopkinson A. Concise review: evidence for CD34 as a common marker for diverse progenitors. *Stem Cells* 2014;32(6):1380-1389.

29 Bhatwadekar AD, Guerin EP, Jarajapu YPR, Caballero S, Sheridan C, Kent D, Kennedy L, Lansang MC, Ruscetti FW, Pepine CJ, Higgins PJ, Bartelmez SH, Grant MB. Transient inhibition of transforming growth factor-beta1 in human diabetic CD34+ cells enhances vascular reparative functions. *Diabetes* 2010;59(8):2010-2019.

30 Abu El-Asrar AM, Nawaz MI, Ahmad A, Siddiquei MM, Allegaert E, Gikandi PW, De Hertogh G, Opdenakker G. CD146/soluble CD146 pathway is a novel biomarker of angiogenesis and inflammation in proliferative diabetic retinopathy. *Invest Ophthalmol Vis Sci* 2021;62(9):32.

31 Nakao S, Ishikawa K, Yoshida S, Kohno RI, Miyazaki M, Enaida H, Kono T, Ishibashi T. Altered vascular microenvironment by bevacizumab in diabetic fibrovascular membrane. *Retina* 2013;33(5):957-963.

32 Suzuma K, Tsuiki E, Matsumoto M, Fujikawa A, Kitaoka T. Retro-mode imaging of fibrovascular membrane in proliferative diabetic retinopathy after intravitreal bevacizumab injection. *Clin Ophthalmol* 2011;5:897-900.

33 Chung EJ, Kang SJ, Koo JS, Choi YJ, Grossniklaus HE, Koh HJ. Effect of intravitreal bevacizumab on vascular endothelial growth factor expression in patients with proliferative diabetic retinopathy. *Yonsei Med J* 2011;52(1):151-157.

34 Han XX, Guo CM, Li Y, Hui YN. Effects of bevacizumab on the neovascular membrane of proliferative diabetic retinopathy: reduction of endothelial cells and expressions of VEGF and HIF-1α. *Mol Vis* 2012;18:1-9.

35 Kohno RI, Hata Y, Mochizuki Y, Arita R, Kawahara S, Kita T, Miyazaki M, Hisatomi T, Ikeda Y, Aiello LP, Ishibashi T. Histopathology of neovascular tissue from eyes with proliferative diabetic retinopathy after intravitreal bevacizumab injection. *Am J Ophthalmol* 2010;150(2):223-229.e1.

36 Hu ZZ, Su Y, Xie P, Chen L, Ji JD, Feng T, Wu SW, Liang K, Liu QH. OCT angiography-based monitoring of neovascular regression on fibrovascular membrane after preoperative intravitreal conbercept injection. *Graefes Arch Clin Exp Ophthalmol* 2019; 257(8):1611-1619.

37 Pattwell DM, Stappler T, Sheridan C, Heimann H, Gibran SK, Wong D, Hiscott P. Fibrous membranes in diabetic retinopathy and bevacizumab. *Retina* 2010;30(7):1012-1016.

38 Zhou T, Che D, Lan YQ, Fang ZZ, Xie JY, Gong HJ, Li CY, Feng J, Hong HH, Qi WW, Ma CQ, Yang ZH, Cai WB, Zhong J, Ma JX, Yang X, Gao GQ. Mesenchymal marker expression is elevated in Müller cells exposed to high glucose and in animal models of diabetic retinopathy. *Oncotarget* 2017;8(3):4582-4594.

39 Hosaka F, Saito W, Kase S, Ishida S. Gliotic opaque posterior hyaloid membrane separation: report of two cases. *BMC Ophthalmol* 2021;21(1):308.

40 Yan XH, Andresen P, Lumi X, Chen QS, Petrovski G. Expression of progenitor cell markers in the glial-like cells of epiretinal membranes of different origins. *J Ophthalmol* 2018;2018:7096326.

41 Aleman-Flores R, Mompeo-Corredera B. Glial cells and retinal nerve fibers morphology in the optic nerves of streptozotocin-induced hyperglycemic rats. *J Ophthalmic Vis Res* 2018;13(4):433-438.

42 Osman I, Wang L, Hu G, Zheng Z, Zhou J. GFAP (Glial Fibrillary Acidic Protein)-positive progenitor cells contribute to the development of vascular smooth muscle cells and endothelial cells-brief report. *Arterioscler Thromb Vasc Biol* 2020;40(5):1231-1238.

43 Krishna Chandran AM, Coltrini D, Belleri M, Rezzola S, Gambicorti E, Romano D, Morescalchi F, Calza S, Semeraro F, Presta M. Vitreous from idiopathic epiretinal membrane patients induces glial-to-mesenchymal transition in Müller cells. *Biochim Biophys Acta BBA Mol Basis Dis* 2021;1867(10):166181.

44 Tan W, Zou JL, Yoshida S, Jiang B, Zhou YD. Increased vitreal levels of interleukin-10 in diabetic retinopathy: a Meta-analysis. *Int J Ophthalmol* 2020;13(9):1477-1483.

45 Vishwakarma S, Gupta RK, Jakati S, Tyagi M, Pappuru RR, Reddig K, Hendricks G, Volkert MR, Khanna H, Chhablani J, Kaur I. Molecular assessment of epiretinal membrane: activated microglia, oxidative stress and inflammation. *Antioxidants* (*Basel*) 2020;9(8):E654.

46 Uemura A, Fruttiger M, D'Amore PA, de Falco S, Joussen AM, Sennlaub F, Brunck LR, Johnson KT, Lambrou GN, Rittenhouse KD, Langmann T. VEGFR1 signaling in retinal angiogenesis and microinflammation. *Prog Retin Eye Res* 2021;84:100954.

47 Cáceres-Del-Carpio J, Moustafa MT, Toledo-Corral J, *et al*. *In vitro* response and gene expression of human retinal Müller cells treated with different anti-VEGF drugs. *Exp Eye Res* 2020;191:107903.

48 Forooghian F, Kertes PJ, Eng KT, Albiani DA, Kirker AW, Merkur AB, Fallah N, Cao SJ, Cui J, Or C, Matsubara JA. Alterations in intraocular cytokine levels following intravitreal ranibizumab. *Can J Ophthalmol* 2016;51(2):87-90.

49 Song S, Yu XB, Zhang P, Dai H. Increased levels of cytokines in the aqueous humor correlate with the severity of diabetic retinopathy. *J Diabetes Complications* 2020;34(9):107641.

50 Fan JW, Shen WY, Lee SR, Mathai AE, Zhang R, Xu GZ, Gillies MC. Targeting the Notch and TGF-β signaling pathways to prevent retinal fibrosis *in vitro* and *in vivo*. *Theranostics* 2020;10(18):7956-7973.